Kininogen–Nitric Oxide Signaling at Nearby Nonexcited Acupoints after Long-Term Stimulation

Ting Wang[1,2,3,7], Geng Zhu[1,4,7], Liyue Qin[1,3,7], Qian Wang[1,7], Chen She[3], Dongsheng Xu[5], Weiwei Hu[1], Kenghuo Luo[1], Ying Lei[3], Yanling Gong[1], Arijit Ghosh[1], Dongni Ma[1], Chun-Lei Ding[1], Bu-Yi Wang[1], Yang Guo[1], Shou-Shan Ma[1], Michihiro Hattori[3], Yutaka Takagi[3], Katsutoshi Ara[3], Kazuhiko Higuchi[3], Xingwang Li[1], Lin He[1], Wanzhu Bai[5], Koichi Ishida[3] and Sheng-Tian Li[1,2,6]

Acupuncture treatment is based on acupoint stimulation; however, the biological basis is not understood. We stimulated one acupoint with catgut embedding for 8 weeks and then used isobaric tags for relative and absolute quantitation to screen proteins with altered expression in adjacent acupoints of Sprague Dawley rats. We found that kininogen expression was significantly upregulated in the stimulated and the nonstimulated adjacent acupoints along the same meridian. The enhanced kininogen expression was meridian dependent and was most apparent among small vessels in the subcutaneous layer. Enhanced signals of nitric oxide synthases, cGMP-dependent protein kinase, and myosin light chain were also observed at the nonstimulated adjacent acupoints along the same meridian. These findings uncover biological changes at acupoints and suggest the critical role of the kininogen–nitric oxide signaling pathway in acupoint activation.

JID Innovations (2021);**1:**100038 doi:10.1016/j.xjidi.2021.100038

INTRODUCTION

Acupuncture has been practiced for over 2,500 years in China, and studies have shown the effectiveness of acupuncture for at least two dozen clinical conditions (Zhang et al., 2015). According to traditional Chinese medicine theory, meridians are the channels through which Qi circulates within the body. Acupoints are specific, mappable points along the body's meridians. At acupoints, Qi is infused into the body surface. Although the use of modern technology has dramatically increased our understanding of the biological basis of acupuncture therapy, the biological mechanisms at local acupoints remain elusive. To date, several molecules related to acupoint stimulation have been identified. Acupoint stimulation activates degranulation of mast cells; excites the afferent nerves; and changes the expression of substance P, 5-hydroxytryptamine, or chemokines at the stimulated location (Carlsson et al., 2006; Chen et al., 2017; He et al., 2017; Zhao, 2008). However, an increased level of nitric oxide (NO) at acupoints (Ma, 2003) or near the location of acupoints (Ha et al., 2012) has been found in healthy volunteers. Furthermore, either manual acupuncture (Ma et al., 2017) or laser acupuncture (Jiang et al., 2017) enhances NO release, which lasts for at least 20 minutes in stimulated acupoints. The question is whether these molecules contribute to acupuncture therapy.

Assuming that full activation of an acupoint leads to the transmission of a signal along its meridian, then one should be able to detect similar biological changes at the stimulated acupoint and the neighboring nonstimulated acupoints on the same meridian. On the basis of this hypothesis, we utilized catgut embedding (CEP) into an acupoint to continuously stimulate an acupoint of Sprague Dawley rats. Then, we used the isobaric tags for relative and absolute quantitation (iTRAQ) technique to screen proteins that similarly changed at the stimulated and neighboring unstimulated acupoints on the same meridian. Among 10 proteins that consistently changed in these acupoints, the most substantially changed protein was kininogen (KNG), which has previously been shown to activate the NO pathway (Schmaier, 2000). Using biochemical and immunofluorescence experiments, the expression of KNG, NO synthase (NOS), cGMP-dependent protein kinase or protein kinase G (PKG), and myosin light

[1]*Bio-X Institutes, Key Laboratory for the Genetics of Development and Neuropsychiatric Disorders (Ministry of Education), Shanghai Jiao Tong University, Shanghai, China;* [2]*Brain Science and Technology Research Center, Shanghai Jiao Tong University, Shanghai, China;* [3]*Kao China Research and Development Center, Shanghai, China;* [4]*Department of Biomedical Engineering, School of Medical Instrument, Shanghai University of Medicine & Health Sciences, Shanghai, China;* [5]*Institute of Acupuncture and Moxibustion, China Academy of Chinese Medical Sciences, Beijing, China; and* [6]*Shanghai Key Laboratory of Psychotic Disorders, Shanghai Jiao Tong University, Shanghai, China*

[7]*These authors contributed equally to this work.*

Correspondence: Sheng-Tian Li, Bio-X Institutes, Key Laboratory for the Genetics of Development and Neuropsychiatric Disorders (Ministry of Education), Shanghai Jiao Tong University, 800 Dongchuan Road, Shanghai 200240, China. E-mail: lstian@sjtu.edu.cn

Abbreviations: CEP, catgut embedding; iTRAQ, isobaric tags for relative and absolute quantitation; KNG, kininogen; MLC, myosin light chain; NO, nitric oxide; NOS, nitric oxide synthase; PKG, protein kinase G; sCEP, sham catgut embedding

Received 16 October 2020; revised 26 March 2021; accepted 27 March 2021; accepted manuscript published online XXX; corrected proof published online XXX

Cite this article as: JID Innovations 2021;1:100038

chain (MLC) were shown to be enhanced at the non-stimulated adjacent acupoints.

RESULTS

Long-term but not short-term CEP stimulation of an acupoint enhanced KNG expression at the adjacent acupoint on the same meridian

We continuously stimulated acupoint YangLingQuan (Gall bladder Meridian of Foot-Shaoyang 34, GB34) of Sprague Dawley rats with CEP into the acupoint once a week for 8 weeks and used the iTRAQ technique to screen for proteins that similarly changed in skin samples of GB34 and the neighboring unstimulated acupoints FengShi (GB31) and HuanTiao (GB30) (Figure 1a and b). The iTRAQ identified 1,514 proteins. Among them, we found 10 proteins that were consistently changed >1.5-fold in these three acupoints in CEP-treated rats compared with those in sham CEP (sCEP)-treated rats, including enhanced expression of KNG, cystatin-A, 60S ribosomal protein L15, N-acetylneuraminate lyase, hypothetical protein isoform 1, and Ig gamma-2C chain C region, and decreased expression of histone H1.2, clusterin, actinin alpha 2, and isoform 2 of haptoglobin (Figure 1c).

KNG can be cleaved to kinins, which trigger the formation of NO by binding to kinin receptors (Choi et al., 2012; Damas, 1994; Emanueli and Madeddu, 2001; Zhang et al., 1997). Given that acupuncture treatment enhances NO levels (Jiang et al., 2017; Ma et al., 2017), it is of interest to investigate whether KNG contributes to the biological mechanism of acupuncture therapy and, if so, whether the function of KNG lies in subsequent changes in NO signaling. Thus, we next conducted a one-time or eight-time CEP treatment at Xuanzhong (GB39), another acupoint on meridian GB, and investigated the KNG expression change at GB34 72 hours after the last CEP treatment. The western blotting results showed that the eight-time but not the one-time CEP treatment enhanced KNG expression when compared with that in the sCEP groups (Figure 2a) (n = 12 for the eight-time treatment group, $P < 0.001$; n = 4 for the one-time treatment group, $P = 0.658$), indicating that long-term but not short-term stimulation of an acupoint enhanced KNG expression at the neighboring acupoints of meridian GB. The detailed western blot experimental results are listed in Table 1.

To verify whether the elevation of KNG levels in non-stimulated adjacent acupoints was a meridian-specific phenomenon, we conducted CEP treatment at acupoint Jimen on meridian Spleen Meridian Foot-Taiyin (SP11), which has the same distance to GB34 as to GB39. In this experiment, we conducted CEP twice a week for 4 weeks. As shown in Figure 2b and Table 1, compared with SP11 (n = 5), the CEP treatment at GB39 (n = 3) significantly increased KNG expression at GB34 ($P = 0.048$). We next conducted an eight-time CEP treatment once a week for 8 weeks at acupoint Yinlingquan (SP6) and investigated the expression of KNG 72 hours after the last CEP treatment at acupoint Sanyinjiao (SP9). As shown in Figure 2c and Table 1, the KNG level was significantly increased by CEP treatment compared with that by sCEP treatment (n = 4 for each group, $P = 0.011$). We also experimented with verifying whether the same stimulation from randomly selected

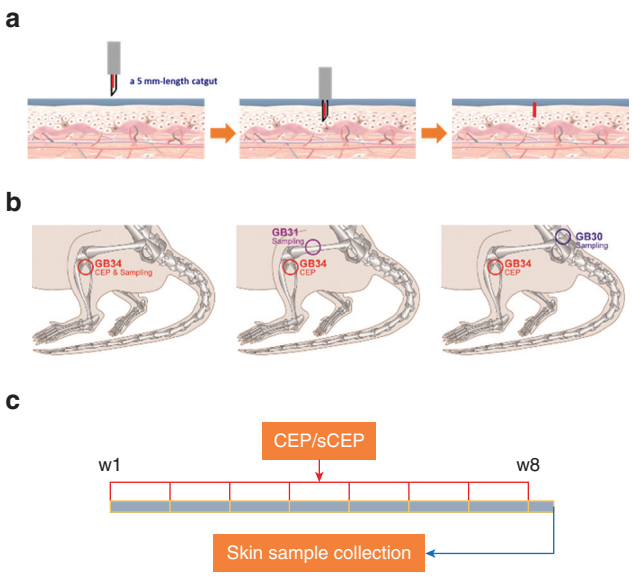

Accession	Description	GB 34	GB 31	GB 30
IPI00886485	Kng1 rat T-kininogen	3.08	1.862	2.182
IPI00209825	Cystatin-A	2.042	2.881	1.533
IPI00231445	60S ribosomal protein L15	1.656	2.721	1.545
IPI00471794	N-acetylneuraminate lyase	1.55	1.587	1.614
IPI00911222	Hypothetical protein isoform 1	1.616	2.758	1.616
IPI00782787	Ig gamma-2C chain C region	3.475	1.645	3.106
IPI00231650	Histone H1.2	0.145	0.343	0.419
IPI00198667	Clusterin	0.499	0.444	0.608
IPI00363022	Actinin alpha 2	0.616	0.381	0.192
IPI00382202	Isoform 2 of haptoglobin	0.377	0.121	0.586

Figure 1. Sustained CEP treatment at GB34 leads to consistent changes of 10 proteins at GB34, GB31, and GB30. (**a, b**) Schematic graphs show the (**a**) CEP treatment procedure and (**b**) treatment and sample collection acupoints. (**c**) The upper panel shows the experimental timeline. The table below shows the iTRAQ results. Compared with the sCEP treatment, the eight-time CEP treatment consistently changes the expression level of 10 proteins at all the three acupoints. The atlas of acupoints used in this paper has been extracted from a previous paper with permission (Wang et al., 2020). CEP, catgut embedding; iTRAQ, isobaric tags for relative and absolute quantitation; sCEP: sham catgut embedding; w, week.

sites would increase KNG expression. We conducted the eight-time CEP or sCEP treatment at SP6 and the eight-time CEP treatment at randomly selected two points in the abdomen, and then the KNG expression at SP9 was compared among these groups. As shown in Figure 2d and Table 1, compared with the sCEP treatment, CEP treatment at SP6 but not the treatment at randomly selected two points in the abdomen enhanced KNG expression (n = 4 for each group, CEP vs. sCEP, $P = 0.014$; CEP treatment at randomly selected two points in the abdomen vs. sCEP, $P = 0.225$), indicating that the enhancement of KNG signaling

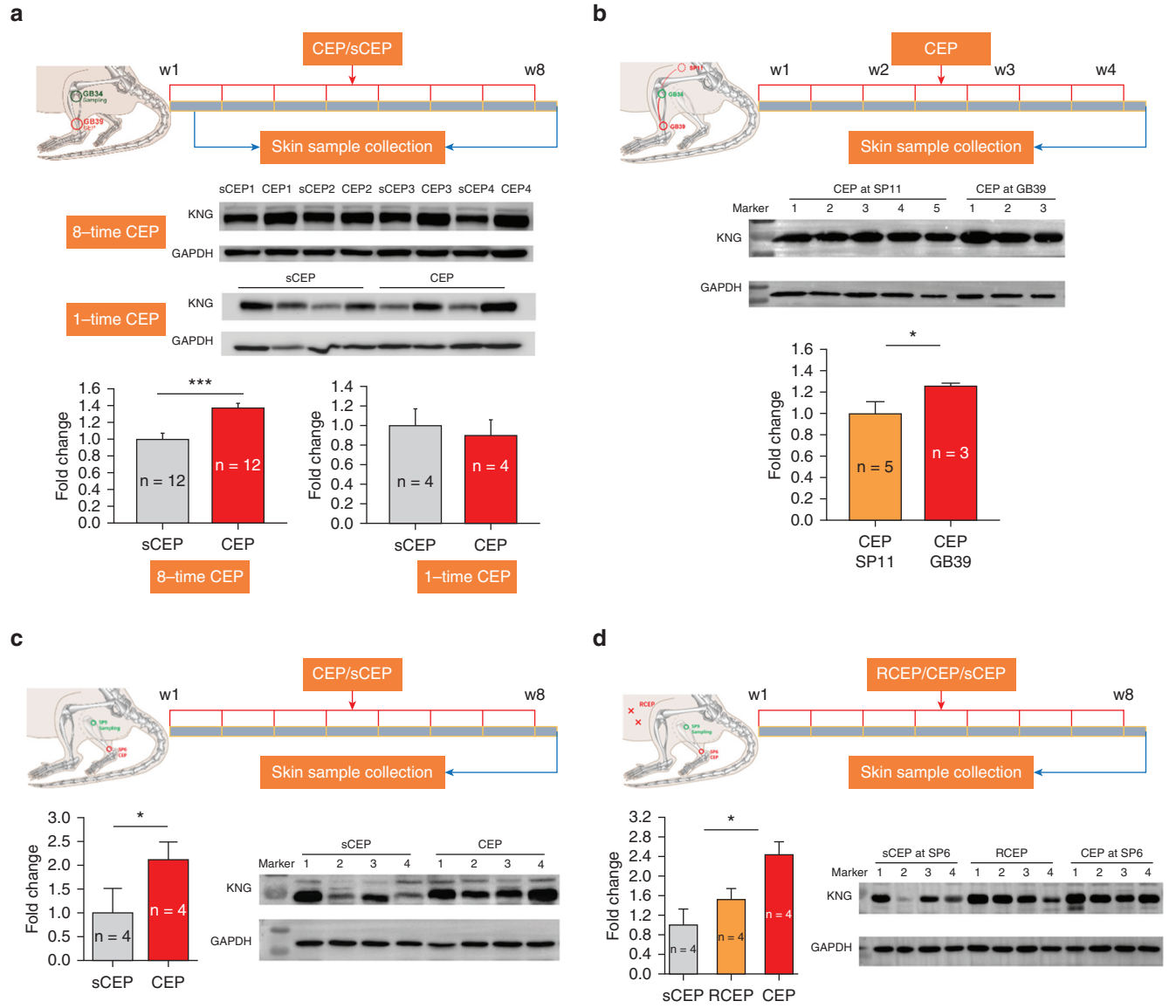

Figure 2. Long-term but not short-term CEP stimulation of an acupoint enhanced KNG expression at the adjacent nonstimulated acupoint on the same meridian. (**a**) Western blotting experiments demonstrate that the eight-time but not one-time CEP treatment at GB39 causes increased expression of KNG at GB34 compared with sCEP treatment. (**b**) Compared with SP11, the eight-time CEP treatment at GB39 significantly increases KNG expression at GB34. (**c**) The eight-time CEP treatment at SP6 results in enhanced expression of KNG at SP9 compared with that of the sCEP treatment. (**d**) The eight-time CEP treatment at SP6 enhances KNG expression at SP9, whereas the eight-time RCEP shows no such effect. Schematic graphs show the treatment and sample collection acupoints and the experimental timeline. Error bars represent standard error. $*P < 0.05$; $***P < 0.001$. CEP, catgut embedding; KNG, kininogen; RCEP, catgut embedding treatment at randomly selected two points in the abdomen; sCEP: sham catgut embedding; w, week.

is not due to systemic effects of CEP treatment, such as systemic circulation.

Then, to verify the locations where KNG levels were enhanced, we performed immunofluorescence staining of skin tissue from GB34 after delivering the eight-time CEP treatment at GB39. Compared with the sCEP group, increased KNG expression was diffused in all epidermis, dermis, and subcutaneous layers, particularly among small vessel structures in the subcutaneous layer in the CEP group (Figure 3a). Similarly, compared with CEP treatment at SP11, the eight-time CEP at GB39 enhanced the KNG signal among small vessel structures in the subcutaneous layer at GB34 (Figure 3b). Compared with sCEP, the eight-time CEP treatment at SP6 enhanced KNG expression among small vessel structures in the subcutaneous layer of SP9 (Figure 3c). Thus, these results indicate that enhancement of KNG signal at an acupoint is a meridian-specific phenomenon.

CEP treatment enhanced the KNG–NO signaling pathway

Studies have shown that acupuncture treatment enhances NO levels (Jiang et al., 2017; Ma et al., 2017). Thus, we next investigated NOS expression. Immunofluorescence staining showed that the expression of endothelial NOS, inducible NOS, and neuronal NOS were most apparent among small vessel structures in the subcutaneous layer in the CEP group compared with that in the sCEP group, both at GB34 (Figure 4a and b) and at SP6 (Figure 4c and d).

Table 1. Statistical Analysis of Western Blotting Experiments

Figure Number	Treatment Points	Treatment Times	Sampling Points	Protein	sCEP	CEP		*P*-Value
Figure 2a	GB39	8	GB34	KNG	1 ± 0.07 (n = 12)	1.37 ± 0.06 (n = 12)		<0.001
		1	GB34		1 ± 0.17 (n = 4)	0.89 ± 0.16 (n = 4)		0.658
Figure 5b		8	GB34	PKG	1 ± 0.06 (n = 12)	1.56 ± 0.12 (n = 12)		<0.001
		8	GB34	MLC	1 ± 0.06 (n = 7)	1.55 ± 0.16 (n = 7)		0.004
Figure 2b	SP11/GB39	8	GB34	KNG		CEP at SP11	CEP at GB39	0.048
						1.00 ± 0.12 (n = 5)	1.26 ± 0.02 (n = 3)	
Figure 2c	SP6	8	SP9	KNG	1 ± 0.25 (n = 4)	2.12 ± 0.18 (n = 4)		0.011
Figure 2d	SP6/RCEP	8	SP9	KNG	sCEP at SP6	CEP at SP6	RCEP	CEP versus sCEP 0.014
					1 ± 0.33 (n = 4)	2.45 ± 0.26 (n = 4)	1.53 ± 0.22 (n = 4)	RCEP versus sCEP 0.225

Abbreviations: CEP, catgut embedding; KNG, kininogen; MLC, myosin light chain; PKG, protein kinase G; RCEP, catgut embedding treatment at randomly selected two points in the abdomen; sCEP, sham catgut embedding.

PKG and MLC, the two molecules involved in biological effects of NO (Choi et al., 2012; Lee et al., 2007; Nakamura et al., 2007; Sharma et al., 2008), were also upregulated 55% and 56%, respectively, at acupoint GB34 by the eight-time CEP treatment at GB39 (Figure 5a and b and Table 1) (PKG, n = 12 for the CEP and sCEP groups, $P < 0.001$; MLC, n = 7 for the CEP and sCEP groups, $P = 0.004$). Similar to the distribution of the NOSs, immunofluorescence staining showed prominent expression of both PKG and MLC among small vessel structures in the subcutaneous layer (Figure 5c).

DISCUSSION

CEP is an acupuncture technique developed at the end of the last century. Although the CEP treatment has been utilized initially for clinical treatment, it is a suitable technique to perform in experimental animals because it can be conducted in anesthetized animals, thereby avoiding the stress induced by restraining the animals, fixation, or other stimulations during manual or electroacupuncture. Stimulation of acupoints with CEP treatment can last for hours to days, allowing more vital stimulation on acupoints than manual and electroacupuncture treatment. Furthermore, CEP treatment quantifies the stimulus intensity by the catgut's length and the frequency of catgut embedding, thus allowing repeatability of the experiment (Ishida et al., 2019).

In this study, eight-time but not one-time CEP treatment at an acupoint enhanced the expression of the KNG–NO signaling pathway at adjacent nonstimulated acupoints along the same meridian of Sprague Dawley rats, thus demonstrating the relationship of KNG to acupoint activation. Depending on the structure and molecular weight, KNG is divided into high molecular-weight KNG (626 amino acids, 88–120 kDa) and low molecular-weight KNG (409 amino acids, 50–68 kDa), which are formed by alternative splicing of *Kng1* in mammals (Moreau et al., 2005). High molecular-weight KNG and low molecular-weight KNG also differ in terms of their susceptibility to cleavage by plasma or tissue kallikreins: whereas the high molecular-weight KNG is cleaved by the plasma kallikreins to produce bradykinin, the low molecular-weight KNG is cleaved by the tissue kallikreins to produce kallidin (Moreau et al., 2005). Bradykinin binds to two receptors: B2R and B1R. Whereas B2R is the constitutively expressed receptor for bradykinin, B1R is upregulated only during inflammatory conditions (Schmaier, 2016). B2R is also known to interact with endothelial NOS, whereas B1R is known to interact with cytokine-inducible NOS (Schmaier, 2016). Therefore, whether enhancement of KNG in acupoints activates NO signals through the action of bradykinin on B1R or B2R remains to be further investigated.

The temporary rise in NO release in stimulated acupoints either by manual or laser acupuncture has been previously reported (Jiang et al., 2017; Ma et al., 2017). In this study, we further showed that long-term stimulation of an acupoint enhanced NOS, PKG, MLC, as well as KNG expression at nonstimulated adjacent acupoints. We wondered how CEP stimulation in one acupoint enhanced KNG/NO signals in nonstimulated neighboring acupoints. Several studies have found that acupuncture improves local circulation (Carlsson, 2002; Hsiao and Tsai, 2008; Jou and Ma, 2009; Loaiza et al., 2002; Tsuchiya et al., 2007). Indeed, KNG (Bhoola et al., 1992; Oza et al., 1990; Schmaier et al., 1988) or NO (Sauzeau et al., 2000; Surks et al., 1999; Tang et al., 2003) is extensively produced from endothelial cells, and NO is well-established as an endothelium-dependent vascular relaxing factor (Huang et al., 1995; Ignarro et al., 1999; Mattagajasingh et al., 2007) through the activation of PKG and MLC (Sauzeau et al., 2000; Surks et al., 1999; Tang et al., 2003). Our results found that KNG and downstream signals were mainly costained with phalloidin. Because phalloidin is the marker of small blood vessels (Lim et al., 2013; Wang et al., 2020), it is highly possible that the long-term CEP stimulation at an acupoint at least leads to the increased expression of KNG–NO signals in vascular endothelial cells of unstimulated neighboring points along the meridian. Nevertheless, it is also possible that sensory nerve activation or release of inflammatory cytokines by CEP treatment takes part in the activation of the KNG–NO signaling pathway. More immunofluorescence studies using specific markers of various cell types are needed to confirm the origin of the enhanced KNG–NO signals.

One limitation of our study is that we did not examine whether the KNG expression was increased near the

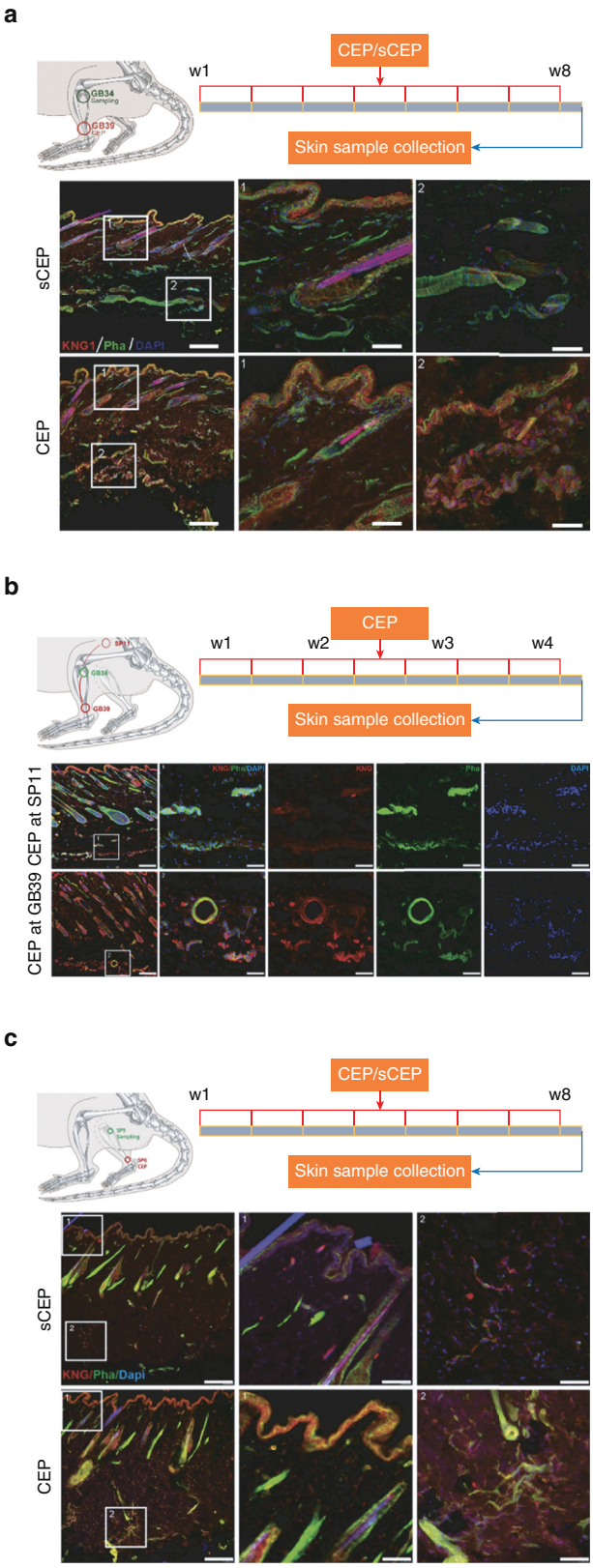

Figure 3. Long-term CEP treatment at an acupoint enhanced KNG signal at the adjacent nonstimulated acupoint on the same meridian.
Immunofluorescence stainings. (**a**) The eight-time CEP treatment at GB39 results in increased KNG signal in all epidermis, dermis, and subcutaneous layers, particularly among the subcutaneous layer's small vessel structures. (**b**) The eight-time CEP treatment at GB39 results in an enhanced KNG signal at GB34 compared with the CEP treatment at SP11, particularly among the subcutaneous layer's small vessel structures. (**c**) The eight-time CEP treatment at SP6 enhanced the KNG signal at SP9. Fluorescent DAPI labels the nuclei, and phalloidin is stained green. Bars = 200 μm (the images at low magnification) and 50 μm (the enlarged images). CEP, catgut embedding; KNG, kininogen; sCEP, sham catgut embedding; w, week.

nonacupoint regions, that is, whether the propagation of the KNG–NO signal by CEP treatment was within the same meridian of the stimulated acupoint. The problem is that histologically, notably different biological structures between acupoints and nonacupoints are unknown. In addition, there is no unified standard of the size of the acupoint. Furthermore, it is difficult to distinguish the acupoint and the para-acupoint areas, especially in small experimental animals, because of the body size limitation. Thus, further investigations with larger animals, where the acupoint and para-acupoint areas can be separated, are needed to explore whether the activation and propagation of the KNG–NO signal is within the same stimulated meridian.

In summary, we show that an acupoint's long-term stimulation enhances the expression of KNG, NOS, PKG, and MLC at nonstimulated adjacent acupoints on the same meridian. Yin and Yang's concept in traditional Chinese medicine is a pair of attributes from ancient Chinese philosophy: Yin and Yang represent opposite aspects of every object and its implicit conflict and interdependence. The Yin meridians are on the ventral and medial regions (e.g., SP), whereas the Yang meridians are located on the body's dorsal and lateral regions (e.g., GB). Thus, the enhancement of KNG–NO signaling among Yang and Yin meridians indicates a common mechanism of acupoints activation. Our findings also suggest the critical role of the KNG–NO signaling pathway in meridian signal transmission (Figure 6) and imply a new direction for the development of alternative acupuncture therapy, for example, application of a plaster coated with NO donor to the skin surface of the acupoints. Revealing the biological changes on these acupoints would help understand the common mechanisms of acupoints activation and meridian signals transduction.

MATERIALS AND METHODS

Animals

Male Sprague Dawley rats aged 6 weeks and weighing 200 ± 10 g from the Shanghai Institute for Biological Sciences (Shanghai, China) were housed in standard colony conditions at ambient temperature between 23 °C and 25 °C with a reversed light/dark cycle of 12 hours to 12 hours (lights off at 9:00 and lights on at 21:00). They had free access to food and water and were allowed to adapt to the environment for at least 1 week before experiments. All experiments were performed according to the guidelines of the Animal Care and Experimentation Committee of Shanghai Jiao Tong University (Shanghai, China). All efforts were made to minimize pain and suffering and to reduce the number of rats used.

CEP treatment

For iTRAQ and western blot tests, rats were randomly divided into two groups: the CEP group and the sCEP group. CEP was performed at the acupoints Yanglingquan (Gall bladder Meridian of Foot-Shaoyang 34, GB34), Xuanzhong (GB39), Yinlingquan (Spleen

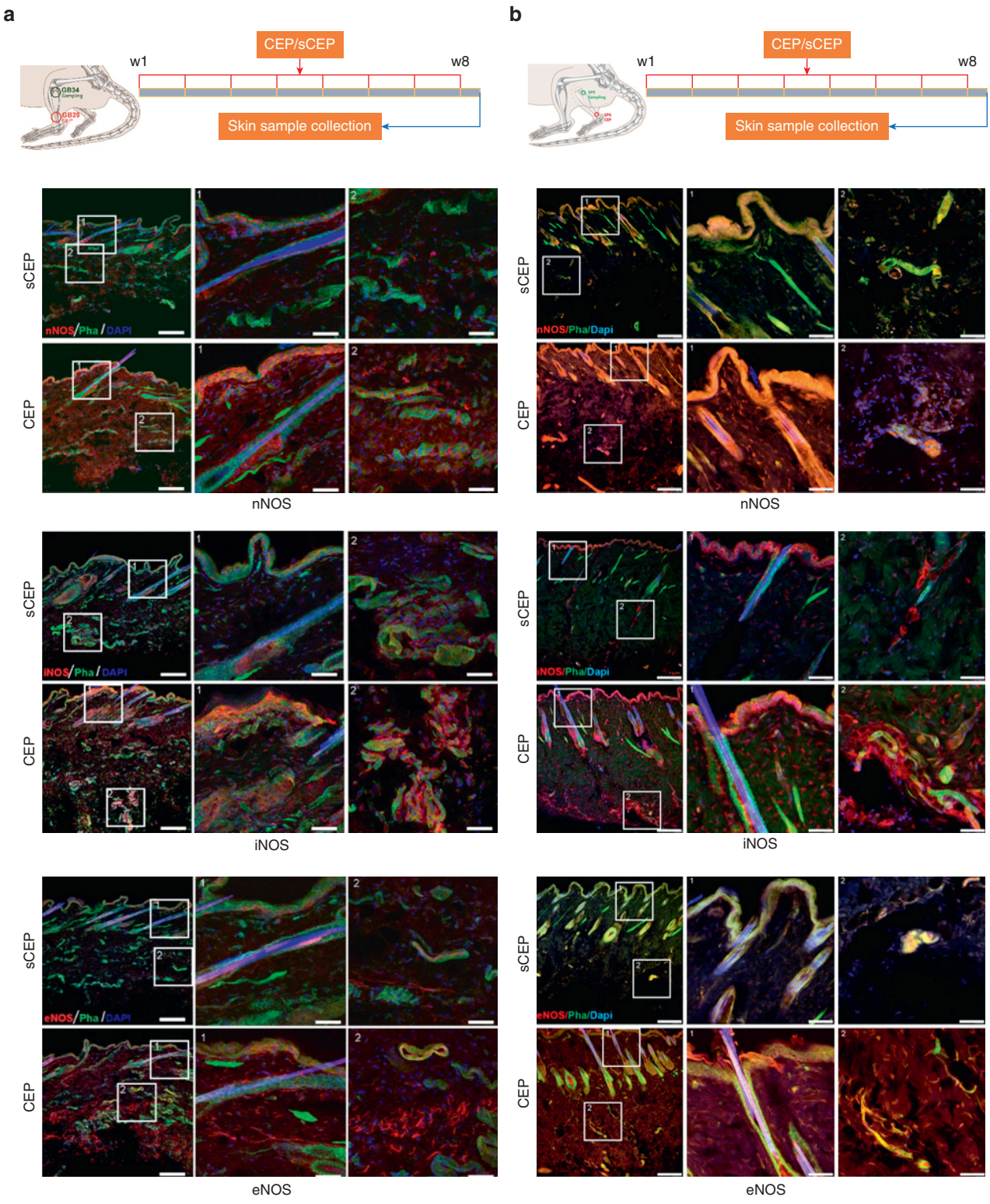

Figure 4. Long-term CEP treatment at an acupoint enhanced NOSs signals at the adjacent non-stimulated acupoint on the same meridian.
Immunofluorescence stainings. (**a**) The 8-time CEP treatment at GB39 results in increased nNOS, iNOS, and eNOS signals at GB34. The schematic graph shows the treatment and sample collection acupoints and the experimental timeline. (**b**) The 8-time CEP treatment at SP6 results in increased nNOS, iNOS, and eNOS signals at SP9. The schematic graph shows the treatment and sample collection acupoints and the experimental timeline. Fluorescent DAPI labels the nuclei, and phalloidin is stained green. Bars = 200 μm (the images at low magnification) and 50 μm (the enlarged images). CEP, catgut embedding; eNOS, endothelial nitric oxide synthase; iNOS, inducible nitric oxide synthase; nNOS, neuronal nitric oxide synthase; NOS, nitric oxide synthase; Pha, phalloidin; sCEP, sham catgut embedding; w, week.

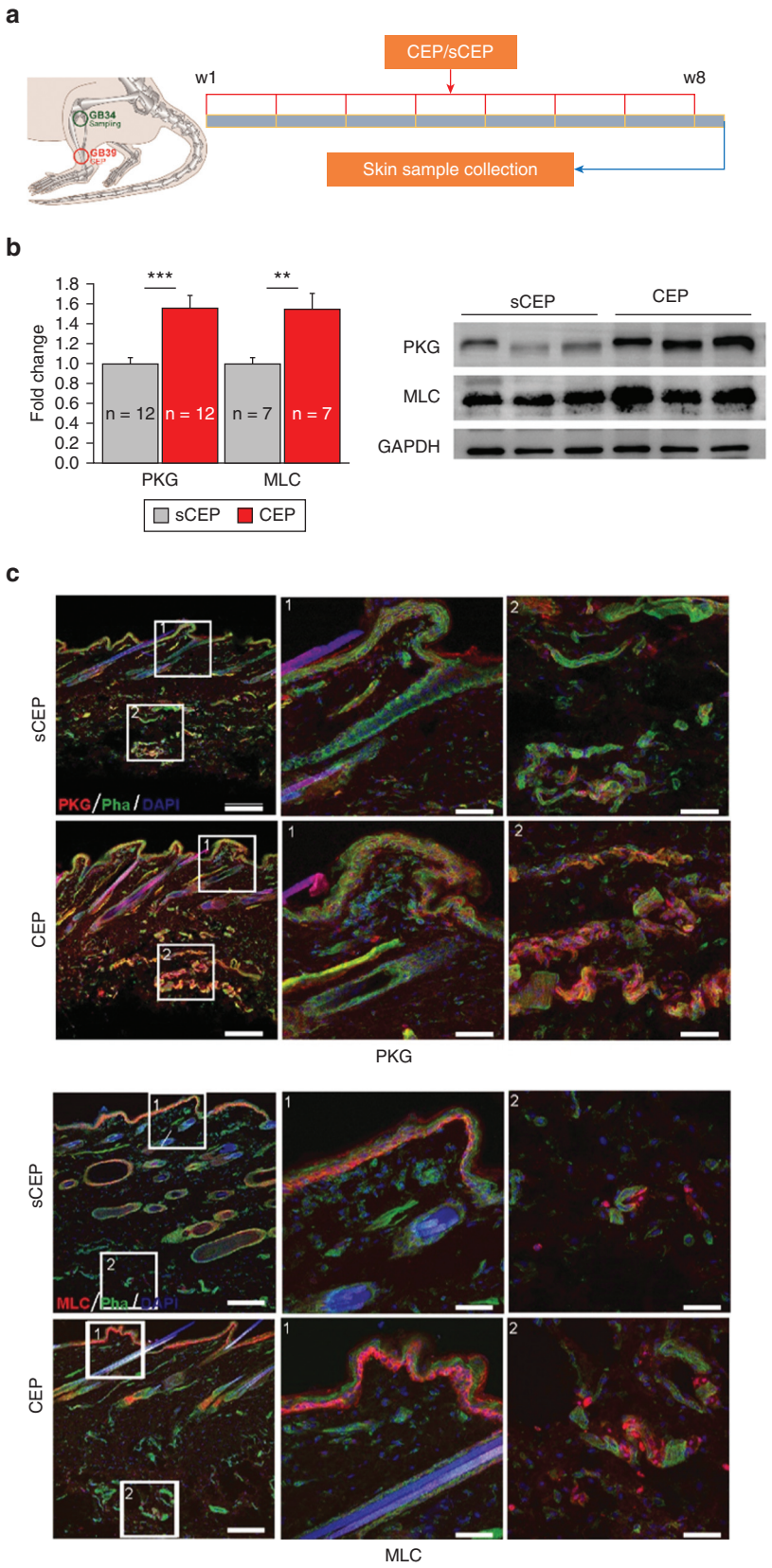

Figure 5. Long-term CEP treatment at GB39 results in the enhanced expression of PKG and MLC at GB34. (**a**) Schematic graphs show the treatment and sample collection acupoints (left) and the experimental timeline (right). (**b**) Western blotting experiments reveal that the w8 CEP treatment at GB39 increases PKG and MLC expressions at GB34 compared with that in the sCEP groups. $^{**}P < 0.01$; $^{***}P < 0.001$. (**c**) Immunofluorescence stainings show that PKG and MLC signals are most obvious in the CEP group in the subcutaneous layer's small vessel structures. Fluorescent DAPI labels the nuclei, and Pha is stained green. Error bars represent standard error. Bars = 200 μm (the images at low magnification) and 50 μm (the enlarged images). CEP, catgut embedding; MLC, myosin light chain; Pha, phalloidin; PKG, protein kinase G; sCEP, sham catgut embedding; w, week.

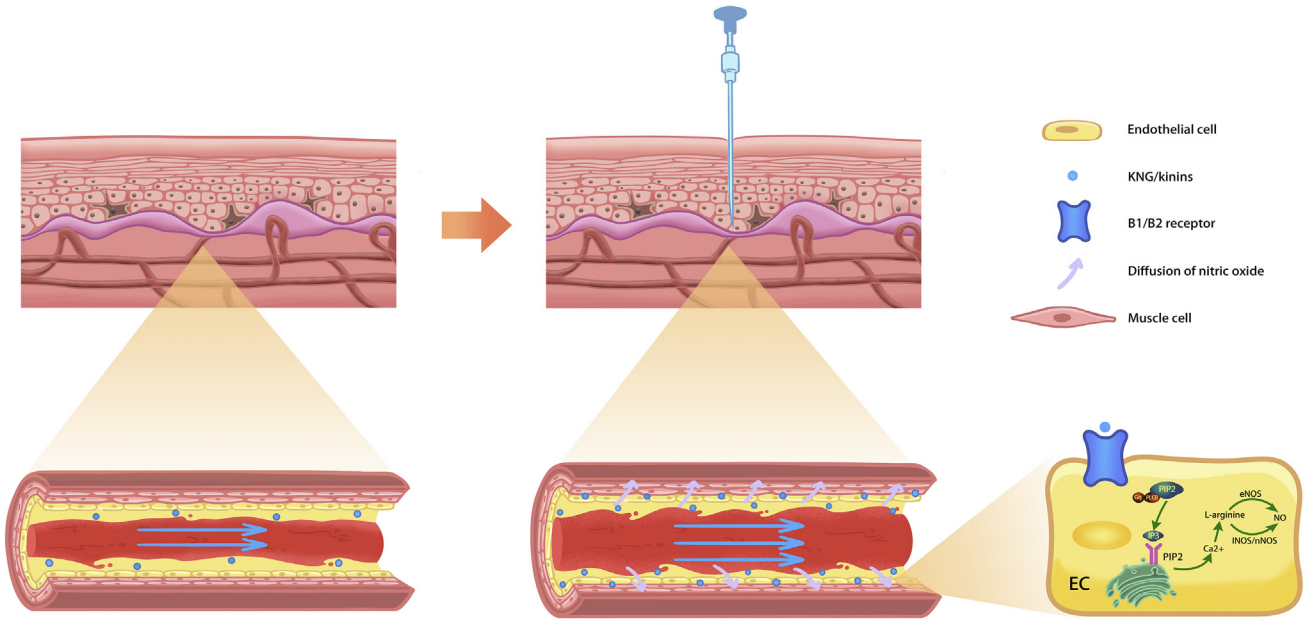

Figure 6. Long-term CEP treatment activates the KNG–NO signaling pathway in acupoints. The diagram illustrates our hypothesis that the sustained stimulation of an acupoint leads to the activation of KNG–NO signals in vascular endothelial cells, which then causes vasodilation and propagation of KNG–NO signals among the meridian. CEP, catgut embedding; KNG, kininogen; NO, nitric oxide.

Meridian of Foot-Taiyin 6, SP6), and Jimen (SP11) on both body sites. We utilized these acupoints as the stimulating or sample-collecting acupoints because these acupoints are often used in animal studies and because they are located on the Yang and Yin meridians, respectively. Revealing the biological changes on these acupoints would help understand the common mechanisms of acupoints activation and meridian signals transduction. Briefly, a 5-mm catgut (Chromic Catgut, 6-0 B60, Shanghai Pudong Jinhuan Medical Products, Shanghai, China) in a disposable sterile syringe needle (0.7 × 32 regular wall, long beveled) was injected into the individual points. Then, a filiform needle (0.35 × 40 mm) was inserted into the syringe to push out and embed the catgut in the acupoint. sCEP was performed by inserting the syringe that does not contain catgut to the acupoints, staying at the point for the same period as CEP treatment, and then withdrawing the syringe. To verify whether the same CEP stimulation from randomly selected sites would have similar effects, we also carried out CEP treatment at randomly selected two points in the abdomen and compared it with the CEP treatment at the acupoints. For immunofluorescence staining, rats were randomly divided into sCEP and CEP groups. CEP and sCEP were performed at GB39 or SP11 on both body sites once a week for 8 weeks. Before each treatment, the individual rat was anesthetized by intraperitoneal injection of sodium pentobarbital (50 mg/kg). Acupoints were determined on the basis of the point map of the experimental animal. The atlas of acupoints used in this paper has been extracted from a previous paper with permission (Xu et al., 2019).

Protein extraction

Skin samples were collected 72 hours after the last CEP/sCEP treatment. Each tissue was ground to powder in liquid nitrogen and then was briefly mixed with 500 μl lysis buffer (210 g Urea, 76 g thiourea, 1 g SDS, 1.2 g Tris were placed in the beaker). We added 250 ml Milli-Q water and place it on the magnetic stirrer overnight (or completely dissolved it). We adjusted the pH of concentrated hydrochloric acid to 8.0–8.5 and fixed the volume to 500 ml with Milli-Q water. Phenylmethylsulfonyl fluoride (BBI, Shanghai, China) and EDTA were added for a final concentration of 1 mM and 2 mM, respectively; after 5 minutes, dithiothreitol was added to a final concentration of 10 mM. The suspension was sonicated at 200 Watts for 15 minutes and then centrifuged at 25,000*g* for 20 minutes. The supernatant was transferred to another tube, 10 mM dithiothreitol was added, and the solution was kept at 56 °C for 1 hour to reduce peptide disulfide bonds. Iodoacetamide (55 mM, Sigma-Aldrich, St. Louis, MO) was added to the solution, and the tube was kept in a dark room for 45 minutes. The solution was incubated in five volumes of chilled acetone for 2 hours at –20 °C and centrifuged again at 25,000*g* for 20 minutes. The pellet was air dried, dissolved in 0.5 M tetraethylammonium bromide (200 μl), and then sonicated at 200 Watts for 15 minutes. The solution was centrifuged at 4 °C at 25,000*g* for 20 minutes, and the protein concentration of the supernatants was determined using a Bradford kit (BGI, Shenzhen, China). Protein from each sample (100 μg) was digested with Trypsin Gold at an enzyme to substrate ratio of 1:20 for 4 hours at 37 °C, and then the digestion step was repeated for 8 hours. After trypsin digestion, the peptide was dried by vacuum centrifugation.

iTRAQ sample labeling

The peptides were reconstituted in 0.5 M tetraethylammonium bromide and then labeled with 8-plex iTRAQ (Applied Biosystems, Foster City, CA), according to the manufacturer's instructions. The peptide mixtures were then pooled and dried by vacuum centrifugation. The pooled mixtures of iTRAQ-labeled peptides were fractionated using strong cation exchange chromatography.

Fractionation by strong cation exchange

For strong cation exchange chromatography using the Shimadzu LC-20AB HPLC Pump system (Shimadzu Scientific Instruments, Columbia, MD) the digested peptides were reconstituted with 4 ml buffer A (25 mM monosodium phosphate in 25% acetonitrile, pH 2.7) and loaded onto a 4.6 × 250 mm Ultremex strong cation exchange column. The peptides were eluted at a flow rate of 1 ml/min

with a gradient of buffer A for 10 minutes, 5−35% buffer B (25 mM monosodium phosphate, 1 M potassium chloride in 25% acetonitrile, pH 2.7) for 11 minutes, and 35−80% buffer B for 1 minute. The elution was monitored by measuring absorbance at 214 nm, and fractions were collected every 1 minute. The eluted peptides were pooled as 12 fractions, desalted by a Strata X C_{18} column, and vacuum dried.

Liquid chromatography with tandem mass spectrometry

For analysis of the iTRAQ-labeled peptide mixtures, each fraction was reconstituted in a particular volume of buffer A (2% acetonitrile, 0.1% formic acid) and centrifuged at 20,000*g* for 10 minutes. In each fraction, the final concentration of peptide was approximately 0.5 μg/μl, on average. The supernatant (10 μl) was loaded on a Shimadzu LC-20AD nano HPLC (Shimadzu Scientific Instruments) by the autosampler onto a 2-cm C_{18} trap column (inner diameter of 200 μm), and the peptides were eluted onto a resolving 10-cm analytical C_{18} column (inner diameter of 75 μm) made in house. The samples were loaded at a rate of 15 μl/min for 4 minutes, and then the 44-minute gradient was run at 400 μl/min starting from 2−35% buffer B (98% acetonitrile, 0.1% formic acid) followed by a 2-minute linear gradient to 80% and maintenance in 80% buffer B for 4 minutes and finally was returned to buffer A for 1 minute. The peptides were subjected to nanoESI followed by tandem mass spectrometry in an LTQ Orbitrap Velos (Thermo Fisher Scientific, Marietta, OH) coupled online to the HPLC. Intact peptides were detected in the Orbitrap at a resolution of 60,000 (full width at half maximum). Peptides were selected for tandem mass spectrometry using higher-energy C-trap dissociation operating mode with a normalized collision energy setting of 45%; ion fragments were detected in the LTQ Orbitrap Velos. A data-dependent procedure that alternated between one mass spectrometry scan followed by eight tandem mass spectrometry scans was applied for the eight most abundant precursor ions above a threshold ion count of 5,000 in the mass spectrometry survey scan with the following dynamic exclusion settings: 2 for repeat counts, 30 seconds for repeat duration, and 120 seconds for exclusion duration. The electrospray voltage applied was 1.5 kV. Automatic gain control was used to prevent overfilling of the ion trap; 1×10^4 ions were accumulated in the ion trap for the generation of higher-energy C-trap dissociation spectra. For mass spectrometry scans, the m/z scan range was 350−2,000 Da.

Database searching and analysis of iTRAQ results

All tandem mass spectrometry samples were analyzed using the Mascot search algorithm (version 2.3.02). Mascot was used to search the international protein index rat protein database (IPI.RAT.fasta.v3.87, ftp://ftp.ebi.ac.uk/pub/databases/IPI/current/) from the European Bioinformatics Institute (Hinxton, United Kingdom) using the following constraints: trypsin as the digestion enzyme; 10 ppm mass tolerance was permitted for intact peptide masses; 0.05 Da was allowed for fragment ions; one missed cleavage was allowed from the trypsin digest; Gln->pyro-Glu (N-term Q), oxidation (M), and iTRAQ (Y) were accepted as potential variable modifications; and carbamidomethyl (C), iTRAQ (N-term), and iTRAQ (K) were taken as the fixed modifications. All identified peptides had an ion score above the Mascot peptide identity threshold. Each protein identification was considered confident with at least one unique peptide. For protein abundance ratios measured using iTRAQ, we set a 1.5-fold change as the threshold and a two-tailed *P*-value of 0.05 to identify significant changes.

Western blotting experiments

At 72 hours after the last CEP/sCEP treatment, skin samples (5 × 5 mm) taken from points GB34, GB31, or GB30 were collected under anesthesia. Skin samples were extracted with RIPA lysis buffer (R0287, Sigma-Aldrich, Shanghai, China) or with Minute Total Protein Extraction Kit (SA-01-SK, Invent Biotechnologies, Eden Prairie, MN) and complete protease inhibitor (4693116001, Roche, Shanghai, China) and phosphatase inhibitor (4906837001, Roche). Tissue lysates were mixed with ×5 loading buffer loaded on a 4–12% SDS polyacrylamide gradient gel and transferred to polyvinylidene fluoride (IPFL85R, Millipore, Darmstadt, Germany) membrane by wet transfer. The blots were blocked in 5% BSA in Tris-buffered saline with Tween and incubated overnight with rabbit anti-KNG1 (1:1,000, ab175386, Abcam, Cambridge, United Kingdom), rabbit KNG1 polyclonal antibody (1:500, 11926-1-AP, Proteintech, Rosemont, IL), rabbit polyclonal anti-PKG antibody (1:1,000, PK002, Enzo Life Sciences, New York, NY), rabbit polyclonal anti-MLC antibody (1:1,000, ENT2839, Elabscience Biotechnology, Wuhan, China), and rabbit anti-GAPDH (1:8,000, ab9485, Abcam). Horseradish peroxidase–conjugated secondary antibodies (1:5,000, 111035003, Jackson ImmunoResearch Laboratories, West Grove, PA) and an ECL Kit (332209, Thermo Fisher Scientific, Shanghai, China) were used to detect protein signals. Membranes were imaged with the ChemiDoc System (Bio-Rad Laboratories, Hercules, CA). Selected images were exported and quantified using ImageJ software 2.0 (National Institutes of Health, Bethesda, MD). GAPDH bands were used for normalization.

Immunofluorescence staining

Skin samples (5 × 5 mm) from individual acupoints on both body sites were collected 72 hours after the 8-week CEP/sCEP treatment. Briefly, anesthetized rats were immediately perfused transcardially with 150 ml of 0.9% saline, followed by 300 ml of 4% paraformaldehyde in 0.1 M PBS (pH 7.4). Full-thickness skin was harvested and stored in 25% sucrose PBS at 4 °C. A series of skin sections were cut at a thickness of 20 μm on a cryostat (Thermo Fisher Scientific, Microm International GmbH, Walldorf, Germany) for immunofluorescence staining. After a brief washing in 0.1 M PBS (pH 7.4), tissue sections were incubated in 0.1 M PBS (pH 7.4) containing 3% normal goat serum and 0.5% Triton X-100 for 30 minutes to block nonspecific binding. Primary antibodies, including rabbit polyclonal anti-KNG1 antibody (1:500, ab175386, Abcam), rabbit polyclonal anti-PKG antibody (1:500, PK002, Enzo Life Sciences), rabbit polyclonal anti-MLC antibody (1:250, ENT2839, Elabscience Biotechnology), rabbit polyclonal anti-eNOS antibody (1:250, ab5589, Abcam), rabbit polyclonal anti-iNOS antibody (1:500, NB300-605, Novus Biologicals, Littleton, CO), and rabbit polyclonal anti-nNOS antibody (1:500, ab76067, Abcam), were incubated overnight at 4 °C. On the following day, after washing three times with 0.1 M PBS, sections were exposed to secondary antibodies, including Goat anti-rabbit Alexa Fluor 594 (1:500, A11037, Molecular Probes, Waltham, MA), followed by Alexa Fluor 488 phalloidin (1:1000; A12379, Enzo Life Sciences) and DAPI (1:50,000, D3571, Molecular Probes). After 2 hours of incubation, sections were washed three times with 0.1 M PBS. Negative controls did not have the primary antibodies added during the staining procedure. During the staining process, the sections were kept inside a black container at 26 °C. Samples were imaged with a confocal imaging system (FV1200, Olympus, Tokyo, Japan).

Statistical analysis

All data are expressed as the mean ± SEM. The comparisons between groups were evaluated using an unpaired Student's *t*-test. Statistical significance was set at $P < 0.05$.

Data availability statement

Datasets related to the mass spectrometry proteomics analysis of this article can be found at http://www.proteomexchange.org, hosted at ProteomeXchange Consortium (dataset identifier PXD024018).

ORCIDs

Ting Wang: http://orcid.org/0000-0003-3414-5446
Geng Zhu: http://orcid.org/0000-0002-9902-5456
Liyue Qin: http://orcid.org/0000-0002-7325-8198
Qian Wang: http://orcid.org/0000-0003-0349-5646
Chen She: http://orcid.org/0000-0001-6850-2507
Dongsheng Xu: http://orcid.org/0000-0002-1963-9432
Weiwei Hu: http://orcid.org/0000-0003-2828-6269
Kenghuo Luo: http://orcid.org/0000-0002-1036-8648
Ying Lei: http://orcid.org/0000-0002-5148-2682
Yanling Gong: http://orcid.org/0000-0002-8713-2262
Arijit Ghosh: http://orcid.org/0000-0001-6408-749X
Dongni Ma: http://orcid.org/0000-0002-9831-4539
Chun-Lei Ding: http://orcid.org/0000-0003-2191-2642
Bu-Yi Wang: http://orcid.org/0000-0001-9451-6347
Yang Guo: http://orcid.org/0000-0001-9900-4885
Shou-Shan Ma: http://orcid.org/0000-0003-3011-2751
Michihiro Hattori: http://orcid.org/0000-0003-2526-6051
Yutaka Takagi: http://orcid.org/0000-0003-2699-8932
Katsutoshi Ara: http://orcid.org/0000-0003-4533-4031
Kazuhiko Higuchi: http://orcid.org/0000-0003-1538-1291
Xingwang Li: http://orcid.org/0000-0002-5903-2774
Lin He: http://orcid.org/0000-0003-1079-1195
Wanzhu Bai: http://orcid.org/0000-0001-6285-7788
Koichi Ishida: http://orcid.org/0000-0001-6293-507X
Sheng-Tian Li: http://orcid.org/0000-0002-2836-3802

AUTHOR CONTRIBUTIONS

Conceptualization: STL; Funding Acquisition: STL, KI; Investigation: TW, CLD, BYW, YGo, QW, WH, YGu, AG, DM, CS, DX, WB, GZ, LQ, YL, MH, YT, KA, KH, XL, LH; Methodology: TW, STL, WB, KI; Project Administration: STL, KI; Resources: STL, KI; Supervision: STL, GZ, YL, WB; Validation: STL, KI; Writing - Original Draft Preparation: STL, TW, GZ, QW; Writing - Review and Editing: STL, XL, LH, KI.

ACKNOWLEDGMENTS

The authors thank Yao Wang for her technical assistance. This study was supported by grants from the National Natural Science Foundation of China (number 81871064), the National Key Research and Development Program of China (2016YFC1201701), the Shanghai Committee of Science and Technology (13dz2260500), and the Innovation Program of Shanghai Municipal Education Commission (2019-01-07-00-02-E00037).

CONFLICT OF INTEREST

KI has been an employee of Kao China Research and Development Center. While KI was assigned to the Kao China Research and Development Center, he was involved in this research as a joint researcher between Shanghai Jiao Tong University and Kao China Research and Development Center. The remaining authors state no conflict of interest.

REFERENCES

Bhoola KD, Figueroa CD, Worthy K. Bioregulation of kinins: kallikreins, kininogens, and kininases. Pharmacol Rev 1992;44:1–80.

Carlsson C. Acupuncture mechanisms for clinically relevant long-term effects–reconsideration and a hypothesis. Acupunct Med 2002;20:82–99.

Carlsson CP, Sundler F, Wallengren J. Cutaneous innervation before and after one treatment period of acupuncture. Br J Dermatol 2006;155:970–6.

Chen B, Li MY, Guo Y, Zhao X, Lim HC. Mast cell-derived exosomes at the stimulated acupoints activating the neuro-immune regulation. Chin J Integr Med 2017;23:878–80.

Choi YJ, Uehara Y, Park JY, Chung KW, Ha YM, Kim JM, et al. Suppression of melanogenesis by a newly synthesized compound, MHY966 via the nitric oxide/protein kinase G signaling pathway in murine skin. J Dermatol Sci 2012;68:164–71.

Damas J. Kallikrein, nitric oxide and the vascular responses of the submaxillary glands in rats exposed to heat. Arch Int Physiol Biochim Biophys 1994;102:139–46.

Emanueli C, Madeddu P. Targeting kinin receptors for the treatment of tissue ischaemia. Trends Pharmacol Sci 2001;22:478–84.

Ha Y, Kim M, Nah J, Suh M, Lee Y. Measurements of location-dependent nitric oxide levels on skin surface in relation to acupuncture point. Evid Based Complement Alternat Med 2012;2012:781460.

He W, Wang XY, Shi H, Bai WZ, Cheng B, Su YS, et al. Cutaneous neurogenic inflammation in the sensitized acupoints induced by gastric mucosal injury in rats. BMC Complement Altern Med 2017;17:141.

Hsiao SH, Tsai LJ. A neurovascular transmission model for acupuncture-induced nitric oxide. J Acupunct Meridian Stud 2008;1:42–50.

Huang PL, Huang Z, Mashimo H, Bloch KD, Moskowitz MA, Bevan JA, et al. Hypertension in mice lacking the gene for endothelial nitric oxide synthase. Nature 1995;377:239–42.

Ignarro LJ, Cirino G, Casini A, Napoli C. Nitric oxide as a signaling molecule in the vascular system: an overview. J Cardiovasc Pharmacol 1999;34:879–86.

Ishida K, Qin L, Wang T, Lei Y, Hu W, Zhu G, et al. Local mechanisms for acupoint sensitization in gall bladder meridian of foot shaoyang-a gene chip study. Acupunct Electrother Res 2019;44:77–87.

Jiang WL, Wei HJ, Guo ZY, Ni YR, Yang HQ, Xie SS. Effects of different-intensity laser acupuncture at two adjacent same-meridian acupoints on nitric oxide and soluble guanylate cyclase releases in human. Microcirculation 2017;24:e12390.

Jou NT, Ma SX. Responses of nitric oxide-cGMP release in acupuncture point to electroacupuncture in human skin in vivo using dermal microdialysis. Microcirculation 2009;16:434–43.

Lee E, Hayes DB, Langsetmo K, Sundberg EJ, Tao TC. Interactions between the leucine-zipper motif of cGMP-dependent protein kinase and the C-terminal region of the targeting subunit of myosin light chain phosphatase. J Mol Biol 2007;373:1198–212.

Lim J, Lee S, Su Z, Kim HB, Yoo JS, Soh KS, et al. Primo vascular system accompanying a blood vessel from tumor tissue and a method to distinguish it from the blood or the lymph system. Evid Based Complement Alternat Med 2013;2013:949245.

Loaiza LA, Yamaguchi S, Ito M, Ohshima N. Electro-acupuncture stimulation to muscle afferents in anesthetized rats modulates the blood flow to the knee joint through autonomic reflexes and nitric oxide. Auton Neurosci 2002;97:103–9.

Ma SX. Enhanced nitric oxide concentrations and expression of nitric oxide synthase in acupuncture points/meridians. J Altern Complement Med 2003;9:207–15.

Ma SX, Lee PC, Anderson TL, Li XY, Jiang IZ. Response of local nitric oxide release to manual acupuncture and electrical heat in humans: effects of reinforcement methods. Evid Based Complement Alternat Med 2017;2017:4694238.

Mattagajasingh I, Kim CS, Naqvi A, Yamamori T, Hoffman TA, Jung SB, et al. SIRT1 promotes endothelium-dependent vascular relaxation by activating endothelial nitric oxide synthase. Proc Natl Acad Sci USA 2007;104:14855–60.

Moreau ME, Garbacki N, Molinaro G, Brown NJ, Marceau F, Adam A. The kallikrein-kinin system: current and future pharmacological targets. J Pharmacol Sci 2005;99:6–38.

Nakamura K, Koga Y, Sakai H, Homma K, Ikebe M. cGMP-dependent relaxation of smooth muscle is coupled with the change in the phosphorylation of myosin phosphatase. Circ Res 2007;101:712–22.

Oza NB, Schwartz JH, Goud HD, Levinsky NG. Rat aortic smooth muscle cells in culture express kallikrein, kininogen, and bradykininase activity. J Clin Invest 1990;85:597–600.

Sauzeau V, Le Jeune H, Cario-Toumaniantz C, Smolenski A, Lohmann SM, Bertoglio J, et al. Cyclic GMP-dependent protein kinase signaling pathway inhibits RhoA- induced Ca2+ sensitization of contraction in vascular smooth muscle. J Biol Chem 2000;275:21722–9.

Schmaier AH. Plasma kallikrein/kinin system: a revised hypothesis for its activation and its physiologic contributions. Curr Opin Hematol 2000;7:261–5.

Schmaier AH. The contact activation and kallikrein/kinin systems: pathophysiologic and physiologic activities. J Thromb Haemost 2016;14:28–39.

Schmaier AH, Kuo A, Lundberg D, Murray S, Cines DB. The expression of high molecular weight kininogen on human umbilical vein endothelial cells. J Biol Chem 1988;263:16327–33.

Sharma AK, Zhou GP, Kupferman J, Surks HK, Christensen EN, Chou JJ, et al. Probing the interaction between the coiled coil leucine zipper of cGMP-dependent protein kinase Ialpha and the C terminus of the myosin binding subunit of the myosin light chain phosphatase. J Biol Chem 2008;283:32860–9.

Surks HK, Mochizuki N, Kasai Y, Georgescu SP, Tang KM, Ito M, et al. Regulation of myosin phosphatase by a specific interaction with cGMP-dependent protein kinase. Ialpha Science 1999;286:1583–7.

Tang KM, Wang GR, Lu P, Karas RH, Aronovitz M, Heximer SP, et al. Regulator of G-protein signaling-2 mediates vascular smooth muscle relaxation and blood pressure [published correction appears in Nat Med 2004;10:105]. Nat Med 2003;9:1506–12.

Tsuchiya M, Sato EF, Inoue M, Asada A. Acupuncture enhances generation of nitric oxide and increases local circulation. Anesth Analg 2007;104:301–7.

Wang J, Xu D, Cui J, Wang S, She C, Wang H, et al. A new approach for examining the neurovascular structure with phalloidin and calcitonin gene-related peptide in the rat cranial dura mater. J Mol Histol 2020;51:541–8.

Xu DS, Zhao S, Cui JJ, Ma TM, Xu B, Yu XC, et al. [A new attempt of re-mapping acupoint atlas in the rat]. Zhen Ci Yan Jiu 2019;44:62–5 [in Chinese].

Zhang CS, Tan HY, Zhang GS, Zhang AL, Xue CC, Xie YM. Placebo devices as effective control methods in acupuncture clinical trials: a systematic review. PLoS One 2015;10:e0140825.

Zhang X, Scicli GA, Xu X, Nasjletti A, Hintze TH. Role of endothelial kinins in control of coronary nitric oxide production. Hypertension 1997;30:1105–11.

Zhao ZQ. Neural mechanism underlying acupuncture analgesia. Prog Neurobiol 2008;85:355–75.